VECTOR PLOTTING AS AN INDICATION OF THE APPROACH TO FLUTTER

E. G. Broadbent — Royal Aircraft Establishment, Farnborough, England

Abstract.

A binary flexure-torsion analysis has been made to check theoretically a method for predicting flutter which depends on plotting vectorially the amplitudes of response relative to the exciting force and extracting the relevant damping rate. The results of this calculation are given in the form of graphs both of the vector plots themselves and of the estimated damping rate against forward speed. The estimated damping rates are compared with calculated values. The method has the advantage that in a flight flutter test damping can be estimated from continuous excitation records: the method is an extension of the Kennedy and Pancu technique used in ground resonance testing.

INTRODUCTION

The measurement of normal modes in a ground resonance test needs an elaborate technique both to ensure that the modes are reasonably orthogonal, and to ensure that no mode is missed. The presence of structural damping presents one of the main difficulties. Kennedy and Pancu have suggested a method of analysing the recordings taken by plotting vectorially the displacements relative to the exciting force. Near circles are obtained for each resonance and practical experience seems to show that this type of plot considerably reduces the likelihood of missing a resonance and also improves the accuracy of determining the resonant frequency. This in itself leads to modes being measured which are a better approximation to the true normal modes than is usually possible from amplitude plots alone. In addition the structural damping can be estimated directly for each resonance.

Because of its success in ground resonance tests the idea has arisen of adapting the technique for flight flutter testing. It is hoped that from the flight test under continuous excitation the resonances might be obtained in the same way as from a ground test, with at the same time estimates of the overall damping at each resonance frequency. Thus a graph of damping rate against airspeed can be obtained from a continuous excitation method of flight flutter testing. In this way it is hoped to obtain the best of two worlds; continuous excitation allows more accurate analysis in the presence of buffeting than is possible from a decaying oscillation, and at the same time damping can be plotted against airspeed; and damping gives a more reliable warning of the approach to flutter than does amplitude response. Near the flutter speed, however, the analysis has to deal with a different type of equilibrium than in a ground resonance test, because the aerodynamic forces are powerful and do not represent a conservative system. In order to see whether this leads to any difficulty in application, a simple flexure-torsion binary example has been worked out in the present paper and analysed by the Kennedy-Pancu method at various forward speeds up to the flutter speed. The dampings are obtained and plotted against airspeed and the results are found to agree well with calculated dampings. Some low speed wind-tunnel tests carried out by Bristol Aircraft Limited show that the method can give results with a high degree of repeatability, even in the presence of buffeting.

THEORY OF THE METHOD

The basis of the theory is outlined here for convenience.

One Degree of Freedom

The equation of motion for one degree of freedom can be written in the form:-

$$a\ddot{q} + e(1 + ig)q = Fe^{i\omega t} \tag{1}$$

for a generalized exciting force $Fe^{i\omega t}$,

where a is an inertia coefficient

e is an elastic coefficient

q is a generalized co-ordinate

g is the phase angle of the restoring force (the damping coefficient).

The steady solution will be motion of the form $e^{i\omega t}$, so we substitute $q = \bar{q}\, e^{i\omega t}$.

Equation (1) now becomes:-

$$[-\omega^2 a + e(1 + ig)]\bar{q} = F \tag{2}$$

We let ω_0 be the natural frequency of the one degree of freedom, i.e., $\omega_0^2 = \frac{e}{a}$ and we obtain:-

$$a[\omega_0^2(1 - \tilde{\omega}^2) + ig\omega_0^2]\bar{q} = F \tag{3}$$

where $\tilde{\omega}^2 = \frac{\omega^2}{\omega_0^2}$

For the purpose of vector plotting $\bar{q}$ is written the form:-

$$\bar{q} = q_r + iq_i \tag{4}$$

For any exciting frequency, ω, the quantities q_r and q_i can now be calculated and plotted on an Argand diagram to give the response vector at that frequency relative to the exciting force; i.e., F is taken to lie along the real axis.

Substituting Equation (4) in Equation (3) and equating real and imaginary parts leads to:-

$$a\omega_0^2[q_r(1 - \tilde{\omega}^2) - q_i g] = F \tag{5}$$

and

$$a\omega_0^2[q_r g + q_i(1 - \tilde{\omega}^2)] = 0 \tag{6}$$

Hence

$$q_r = \frac{F}{a\omega_0^2}\left[\frac{1 - \tilde{\omega}^2}{(1 - \tilde{\omega}^2)^2 + g^2}\right] \tag{7}$$

and

$$q_i = \frac{F}{a\omega_0^2}\left[\frac{-g}{(1 - \tilde{\omega}^2)^2 + g^2}\right] \tag{8}$$

As ω is varied the locus of points (q_r, q_i) is a smooth curve obtained by eliminating $\tilde{\omega}$ from these two equations:-

$$\frac{q_r^2}{q_i^2} = -\frac{F}{a\omega_0^2 q_i g} + 1 \tag{9}$$

or

$$q_r^2 + q_i^2 + \left(\frac{F}{a\omega_0^2 g}\right)q_i = 0 \tag{10}$$

This is the equation of a circle with its diameter lying on the negative imaginary axis and passing through the origin (see Figure 1).

The Position of Resonance

Resonance occurs when $\tilde{\omega} = 1$ and from Equation (7) $q_r = 0$, i.e., the vector OC on Figure 1 represents the amplitude at resonance. We can obtain a relation between the rate of change of frequency along the curve at resonance and the damping g, so that if the curve itself is obtained from measurements on a structure of unknown damping, the damping can be estimated.

Consider the point D in Figure 1 when the frequency is $\omega_0 + \delta\omega$. At D

$$\frac{q_r}{q_i} = \tan\frac{\theta}{2} \tag{11}$$

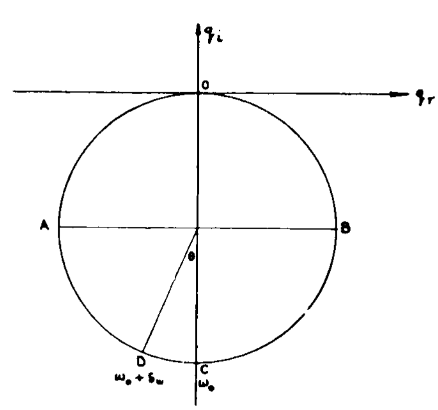

Figure 1. Vector Diagram for One Degree of Freedom — Hysteresis Damping

$$= \frac{1 - \tilde{\omega}_D^2}{g} \tag{12}$$

from Equations (7) and (8).

Hence

$$g = \frac{\delta\omega}{\omega_0}\left(2 + \frac{\delta\omega}{\omega_0}\right) \cot\frac{\theta}{2} \tag{13}$$

It can be seen from Equation (13) that if $\frac{\delta\omega}{\omega_0}$ is small, equal angles will be subtended by equal frequency increments on either side of the resonance. In the particular case when $\theta = \frac{\pi}{2}$ we have:-

and when $\theta = -\frac{\pi}{2}$

$$\left.\begin{aligned} \tilde{\omega}_A^2 &= 1 + g = \frac{\omega_A^2}{\omega_0^2} \\ \tilde{\omega}_B^2 &= 1 - g = \frac{\omega_B^2}{\omega_0^2} \end{aligned}\right\} \tag{14}$$

Hence

$$2g = \frac{\omega_A^2 - \omega_B^2}{\omega_0^2}$$

and

$$2 = \frac{\omega_A^2 + \omega_B^2}{\omega_0^2} \tag{15}$$

Whence

$$g = \frac{\omega_A^2 - \omega_B^2}{\omega_A^2 + \omega_B^2} \tag{16}$$

$$\approx \frac{(\omega_A - \omega_B)}{2\omega_0}$$

It is common practice in this country to express the damping as a percentage of the critical damping. As long as the damping is small, g can be directly related to the percentage of critical damping which is derived from the concept of velocity damping: i.e., the appropriate differential equation is:-

$$a\ddot{q} + d\dot{q} + eq = Fe^{i\omega t} \tag{17}$$

Comparing this with equation (1)

$$d\dot{q} = e\, i\, g\, q \tag{18}$$

and substituting $q = \overline{q}\, e^{i\omega t}$

$$i\omega d = ieg \tag{19}$$

Hence

$$g = \frac{\omega d}{e} \tag{20}$$

But $d = 2\frac{c}{c_c}\sqrt{ae}$ where $\frac{c}{c_c}$ is the fraction of critical damping:-

Hence

$$g = 2\frac{\omega}{\omega_0}\left(\frac{c}{c_c}\right) \tag{21}$$

so that at resonance

$$g = 2\frac{c}{c_c} = \frac{d}{\sqrt{ae}} \tag{22}$$

It should be noted that if the damping is of the form given by Equation (17) the locus of points (q_r, q_i) is no longer a circle; the steady solution will be motion of the form $e^{i\omega t}$, and substituting $q = \overline{q}\, e^{i\omega t}$ the equation becomes:-

$$(-a\omega^2 + di\omega + e)\bar{q} = F \tag{23}$$

Proceeding as before we obtain:-

$$q_r = \frac{F}{a\omega_0^2}\, \frac{1 - \tilde{\omega}^2}{(1 - \tilde{\omega}^2)^2 + \tilde{\omega}^2\bar{g}^2} \tag{24}$$

and

$$q_i = \frac{-F}{a\omega_0^2}\, \frac{\tilde{\omega}\bar{g}}{(1 - \tilde{\omega}^2)^2 + \omega^2\bar{g}^2} \tag{25}$$

Here $\bar{g} = \frac{d}{\sqrt{ae}}$ so that the two systems represented by Equations (1) and (23) will have the same properties at resonance if $g = \bar{g}$. The vector q defined by Equations (24) and (25) now describes a quartic curve starting at the point $\left(\frac{F}{a\omega_0^2}, 0\right)$ when $\omega = 0$ and finishing at the origin when $\omega \to \infty$; any other branches are for unreal frequencies. In practice for small values of g the curve is indistinguishable from a circle except at low frequencies; this is shown in Figure 2 where the circle of Equations (7) and (8) is compared with the quartic of Equations (24) and (25).

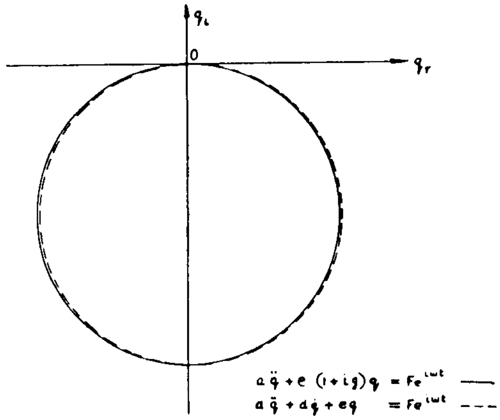

Figure 2. Vector Diagram for One Degree of Freedom — Comparison Between Hysteresis and Velocity Damping

Two Degrees of Freedom

Kennedy and Pancu suggest that with N degrees of freedom there will be N near circles. For any particular resonance, the best circle is put through the points and the resonance is given by the minimum $\frac{\delta\omega}{\omega s}$, where s represents distance along the curve. If equal increments of ω are taken the greatest change of phase gives the resonance. The damping (g) can then be extracted as for one degree of freedom.

Because this method appears to be the best way of estimating damping in ground resonance tests, it has been suggested that it might well be extended to the estimation of damping in a flight flutter test, where continuous excitation is being employed. The method may be difficult when the dampings are high at medium flight speeds, but should improve again for low damping near the flutter speed. The difference between the flight condition near the flutter speed and the ground condition, where the damping is low in each case, is that in flight there will be large asymmetric couplings arising from the aerodynamic forces. It was decided to see how important these were in practice by calculating the response of a simple binary example at various speeds up to the flutter speed.

BINARY EXAMPLE

Basic Data:

Geometry

For simplicity a 2-dimensional rigid wing, restrained by springs in vertical translation and pitch was considered. The two degrees of freedom are:

Vertical translation: $z = cq_1$ (representing wing flexure)

Pitch: $\alpha = q_2$ (representing wing torsion)

in general $z = cq_1 + xq_2$

The axis of pitch is at the half chord.
The axis of centre of gravity is at the half chord.

Since the modes are uncoupled at zero flight speed they are normal modes and the frequency ratio is $\omega_z : \omega_\alpha :: 0.4676:1$.

Structural damping at a value of $g = 0.02$ is assumed to be present in each degree of freedom. It is assumed that displacements to be recorded in flight tests are linear displacements at the half chord, quarter chord and leading edge and the angle of pitch. Thus the first and last of these 'pickups' give measurements proportional to the generalized co-ordinates q_1 and q_2 respectively. Finally it is assumed that the excitation is linear vertical excitation applied at the quarter chord.

Wing Flutter

The aerodynamic derivatives are assumed to be constant both with the frequency parameter and forward speed, i.e., any Mach number effect is neglected.

The equations for free oscillation can be written in the form:-

$$\begin{bmatrix} -14.04\nu^2 + 1.96 v\nu i + (1 + 0.02i) y_0 & 0.68 v\nu i + 2.25 v^2 \\ -.49 v\nu i & -0.8906\nu^2 + 0.24 v\nu i - .565 v^2 + .29 (1 + 0.02i) y_0 \end{bmatrix} \begin{bmatrix} q_1 \\ q_2 \end{bmatrix} = 0 \qquad (26)$$

where V_c = flutter speed

$$\nu = \frac{\omega_c}{V_c}$$

$$v = \frac{V}{V_c}$$

$$y_o = \frac{E_{11}}{\rho V_c^2 s c^2}$$

c is the wing chord

s is the wing span

The equations were solved for y_o with v = 1 (corresponding to the critical flutter speed), and gave $y_o = 2.92$ and $\nu = 0.666$.

From a knowledge of y_o it is possible to relate any known E_{11} (the spring restraint against vertical translation) to an actual flutter speed (V_c), knowing the dimensions. Here, however, we are only interested in the relative speeds, i.e., v, the fraction of V_c.

Response Calculations

With the excitation at the quarter chord and after the substitution for y_o = 2.92, Equation (26) becomes:-

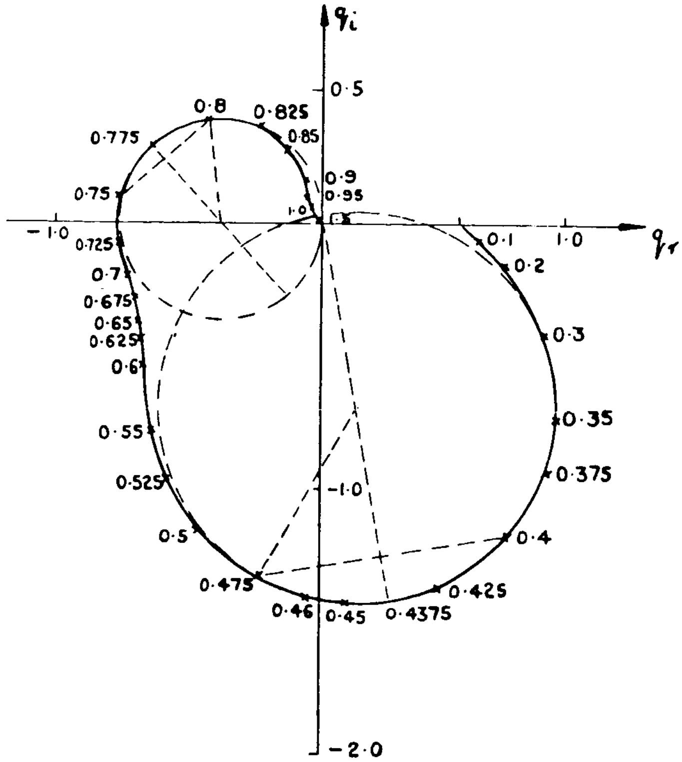

Figure 3. Vector Diagram for Binary Example: v = 0.75, displacement 1

$$\begin{bmatrix} (-14.04\nu^2 + 2.92) + (1.96v\nu + 0.0584)i & 2.27v^2 + 0.63v\nu i \\ -.49v\nu i & (-.8906\nu^2 - 0.565v^2 + 0.8468) + (0.24v\nu + 0.016936)i \end{bmatrix} \begin{bmatrix} q_1 \\ q_2 \end{bmatrix} = \begin{bmatrix} 1 \\ -0.25 \end{bmatrix} F \qquad (27)$$

where F is an arbitrary force level. For simplicity F is taken to be unity in the calculation which follows. Values of v = 0, 0.25, 0.5, 0.75, 0.9 and 1.0 were chosen, and in each case q_1 and q_2 were calculated for a set of increments in ω. Assuming perfect accuracy of recording the measurements taken in flight from the four 'pickups' (half chord, quarter chord, leading edge, pitching angle) would be q_1, $q_1 - 1/4q_2$, $q_1 - 1/2q_2$, q_2.

These quantities were plotted vectorially and the frequencies and rates of decay were estimated from the near circles; a typical example is shown in Figure 3 for pickup 1 at 3/4 of the flutter speed.

Comments on Figures

The change in character of each vector diagram as the forward speed is increased is indicated in Figures 4 to 7. Consider first Figure 4 for displacement 1, i.e. the displacement of the first pickup (see above) which gives a direct measure of the first co-ordinate in the calculation. At zero speed the co-ordinates are normal co-ordinates so that the vector diagram results in a single pure circle with a resonance frequency given by ω = 0.456. As speed is increased the size of the circle reduces (the same scale has been kept throughout each of Figures 4 to 7, although of course different scales were used to estimate frequency rates of decay in practice) and a small secondary circle starts to appear near the origin. This second circle occurs at the frequency of the pitching mode which is now beginning to couple slightly with the bending mode due to the presence of the aerodynamic forces. The new circle continues to increase in size until at a speed of nine tenths of the flutter speed it is the greater of the two. The last diagram in this series is drawn for the flutter speed itself at which one of the circles must have increased indefinitely in size. This is in fact the new circle corresponding to the higher frequency.

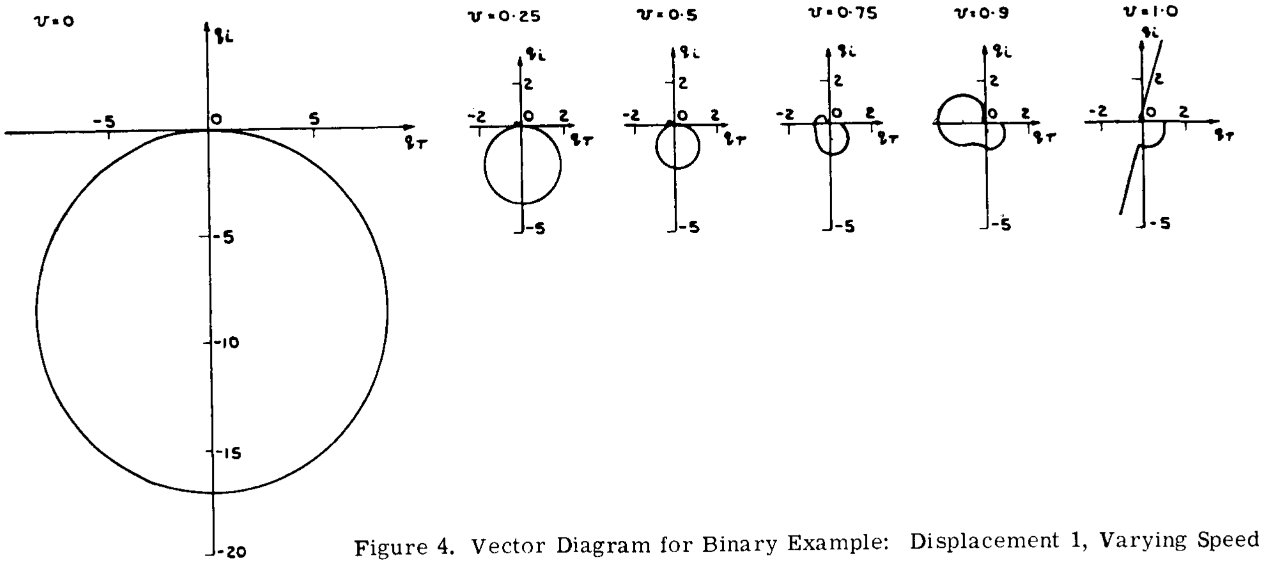

Figure 4. Vector Diagram for Binary Example: Displacement 1, Varying Speed

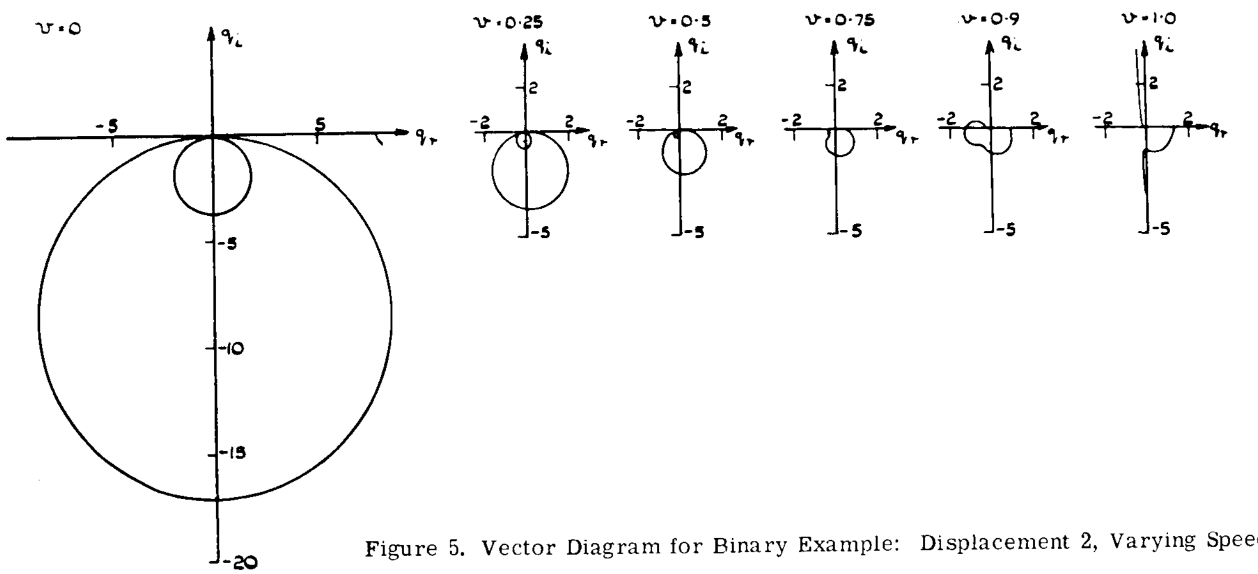

Figure 5. Vector Diagram for Binary Example: Displacement 2, Varying Speed

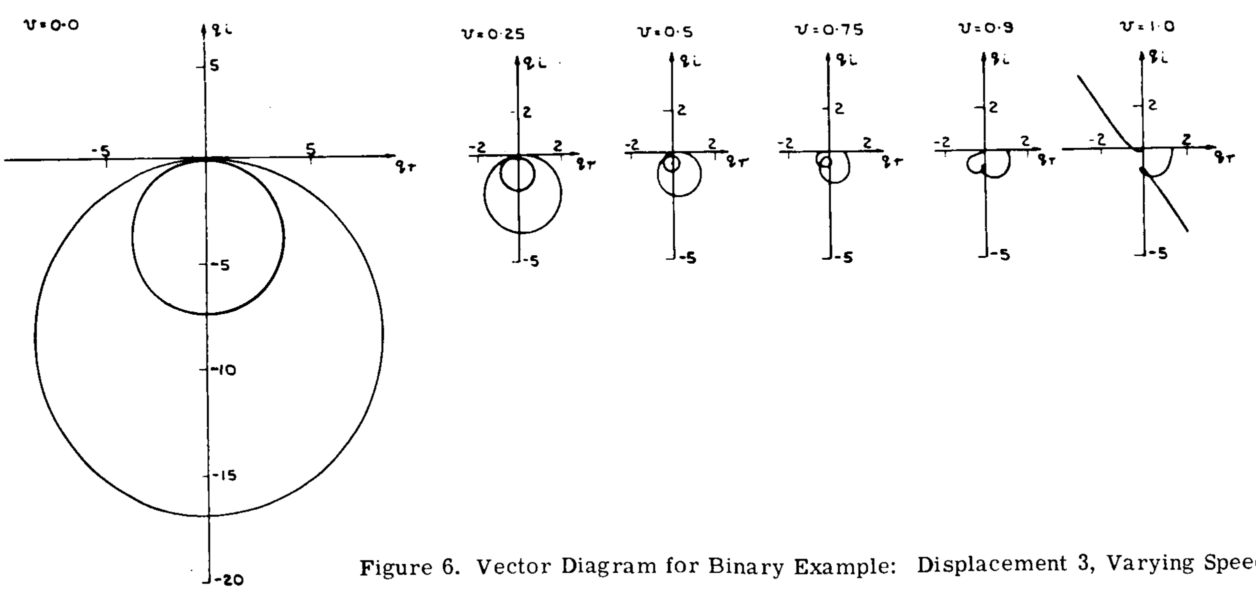

Figure 6. Vector Diagram for Binary Example: Displacement 3, Varying Speed

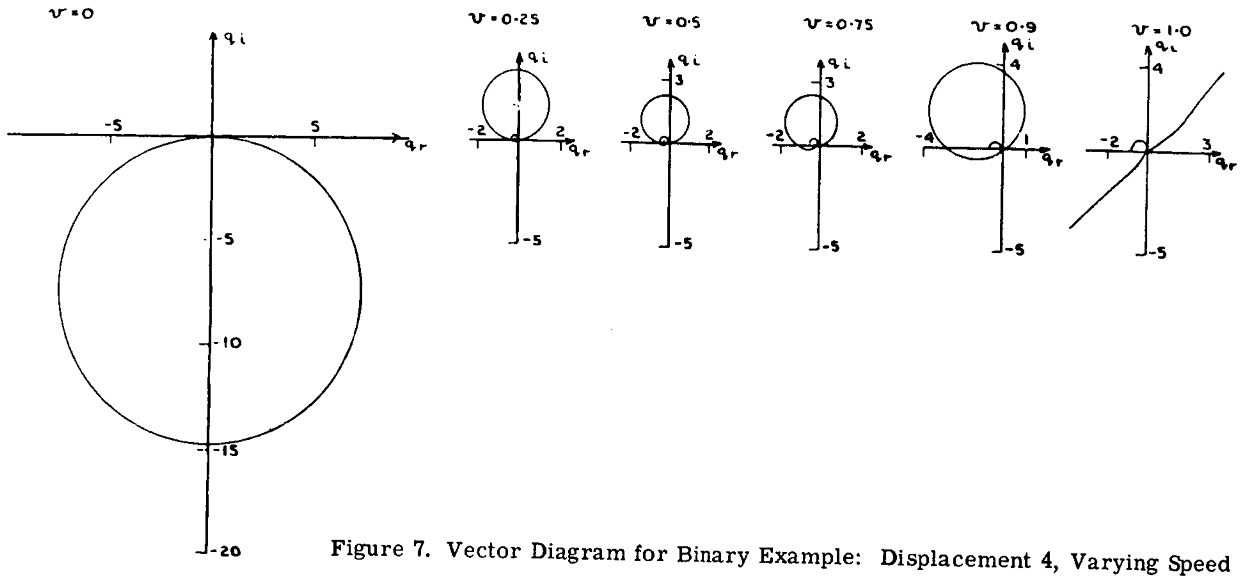

Figure 7. Vector Diagram for Binary Example: Displacement 4, Varying Speed

Figure 5 gives the diagrams for displacement 2, the quarter chord, which shows two circles even at zero speed; neither of these circles are perfect although the error is not detectable on the scale shown. Both circles reduce with increasing airspeed for a time and the smaller (corresponding to the higher frequency) changes its position relative to the origin. Ultimately, as before, the higher frequency circle increases in size to an indefinite extent at the flutter speed. Similar sequences are shown for the other pickups in Figures 6 and 7, although in the last figure the higher frequency circle remains the larger throughout.

Estimation of Damping in Flight and Conclusion

As outlined in paragraph 2 we estimate the damping $\frac{c}{c_c}$ from the circles. Near each resonance suitable equal increments in frequency are chosen, and these are marked on the curves of Figure 3. The actual resonance is picked out from the figures by using a pair of dividers to get the maximum phase change. In this example there was never any difficulty in putting a circle through the points (a typical circle is shown in Figure 3) and the damping was estimated from convenient increments of frequency as can be seen from the construction on Figure 3.

The damping as obtained from each pickup was then plotted against forward speed, and the results are shown in Figure 8. Since our example is completely specified mathematically, the dampings can also be calculated exactly. In Figures 9 and 10 the calculated roots are plotted and compared with the estimates from each of the four 'pickups'. Figure 9A, shows the change in frequency of the lower frequency with forward speed and Figure 9B, shows the change in damping: Figures 10A and B give the corresponding results for the higher frequency root, which is the one that leads to flutter at v = 1.0. The agreement in

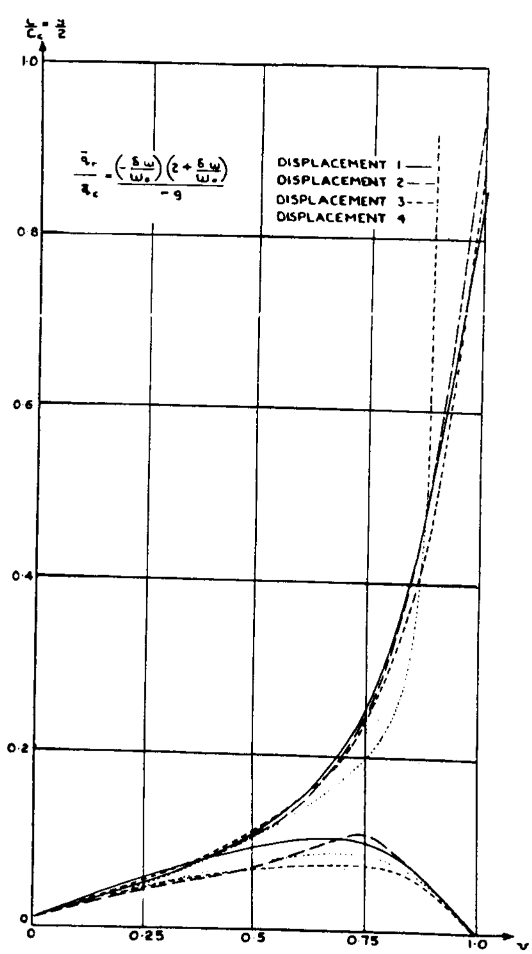

Figure 8. Damping Estimates from the Vector Diagrams Against Forward Speed

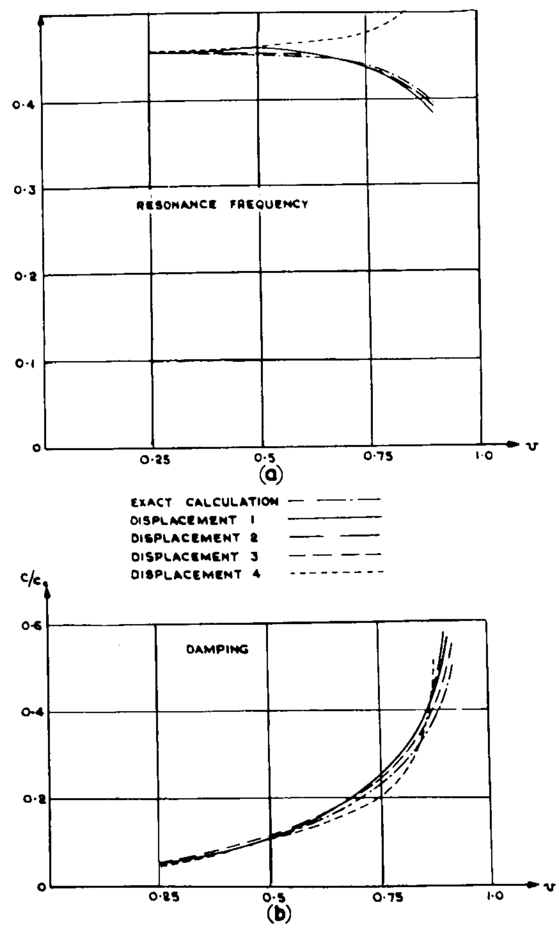

Figure 9. Comparison Between Estimates of Damping and Frequency, and Exact Calculation, Bending Mode

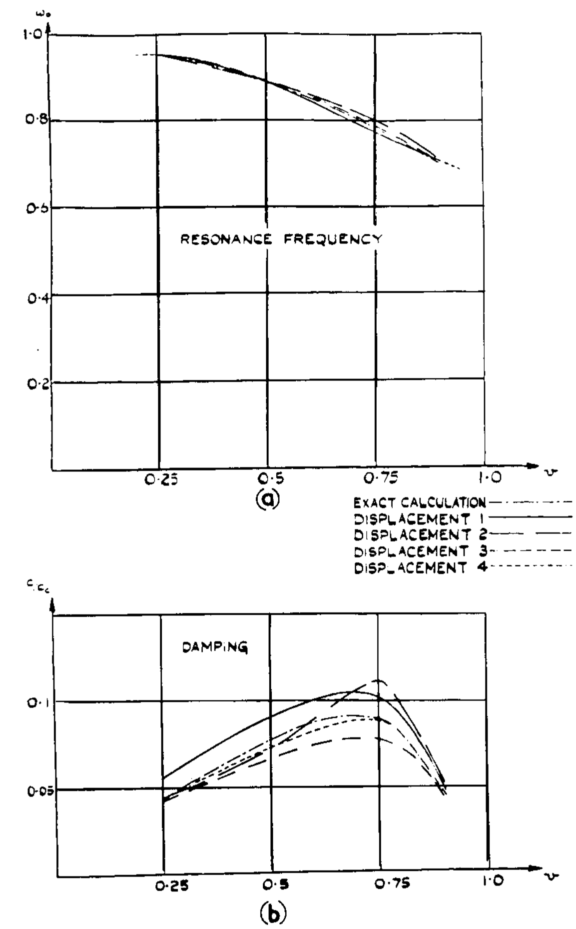

Figure 10. Comparison Between Estimates of Damping and Frequency, and Exact Calculation, Torsion Mode

general between the different estimaes and the calculated values is very good. The only serious error in the lower frequency root is obtained from the rotational 'pickup'; this seems to give the wrong trend of frequency with speed when the damping exceeds 10% of critical – a condition which would in any case be unimportant in practice. For the higher frequency root the accuracy is good throughout, and best for this same rotational pickup, as might be expected on qualitative grounds. Any of the pickups, however, would give a good prediction of flutter speed (see Figure 10B) provided the speed increments chosen were not too large.

From flight measurements in practice one could scarcely hope to get such a consistent set of results as has been obtained from the estimates in this simple binary example. On the other hand the example does suggest that the method is sound in principle so that if there are practical arguments which favour recording from continuous excitation rather than decaying oscillations the Kennedy and Pancu type of analysis is likely to provide good results. It may well be however, that with many degrees of freedom present, as on real aircraft, the choice of pickup position is more important than in the binary example. In general the flight analysis would be carried out for two or three pickups as a normal safety precaution.

RESULTS FROM A LOW SPEED WIND-TUNNEL MODEL

The method outlined above has been applied by Bristol Aircraft Limited to a wind-tunnel model designed to investigate flutter of a T-tail configuration. Figure 11 shows a typical vector diagram at a forward speed that is about 83% of the extrapolated flutter speed. The diagram is for the mode which starts at zero speed as tailplane fundamental symmetric torsion, and which provides the main pointer to the critical flutter condition as did wing pitch in the theoretical example of section 3. The experimental results are consistent and define a very good circle. Figure 12 shows the variation in frequency and damping with airspeed of the fundamental bending mode of the tailplane and Figure 13 gives the corresponding results for the fundamental torsion mode*. The graph of Figure 13 can be extrapolated to the flutter speed.

It is not the purpose of this paper to deal with the experimental technique involved but one or two points should be made. It is necessary to have a phase meter available that gives accurate readings in the presence of buffeting. The instrument used by Bristols measures in-phase and quadrature components, and is arranged to descriminate against noise (as in a wattmeter type of phasemeter). It can give an accuracy of about 5% even with a signal to noise ratio as low as unity. The rate of sweep of the exciter (in terms of frequency) is determined by trial and error, and a satisfactory rate will depend on the damping in each case. The frequency control of the exciter must be accurate, i.e., high short term stability is required, and in practice at low dampings the frequency increments may need to be as small as 0.4% in order to get a reliable measure of the damping.

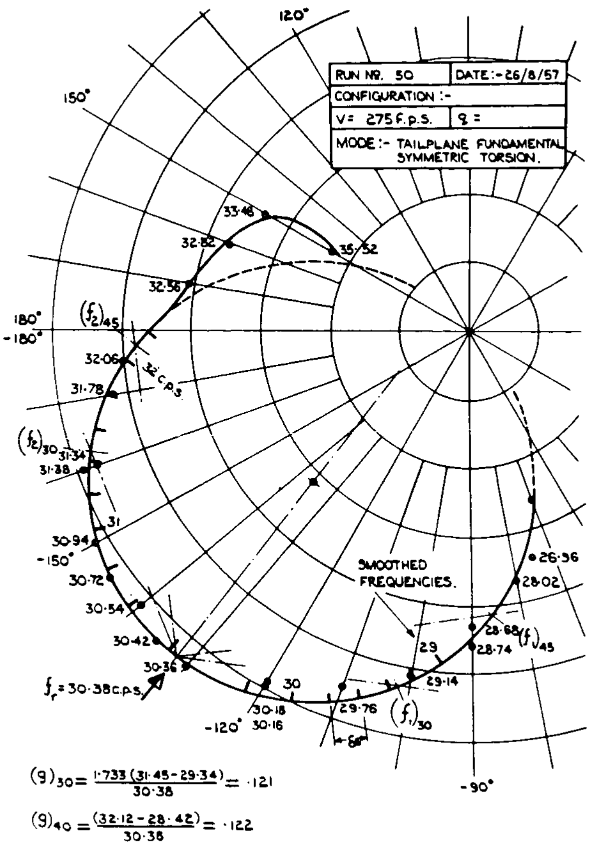

Figure 11. Example of Phase Against Amplitude Plot with Damping Analysis

*These terms are used for descriptive purposes only: in practice, of course, the modes change shape under the aerodynamic forces.

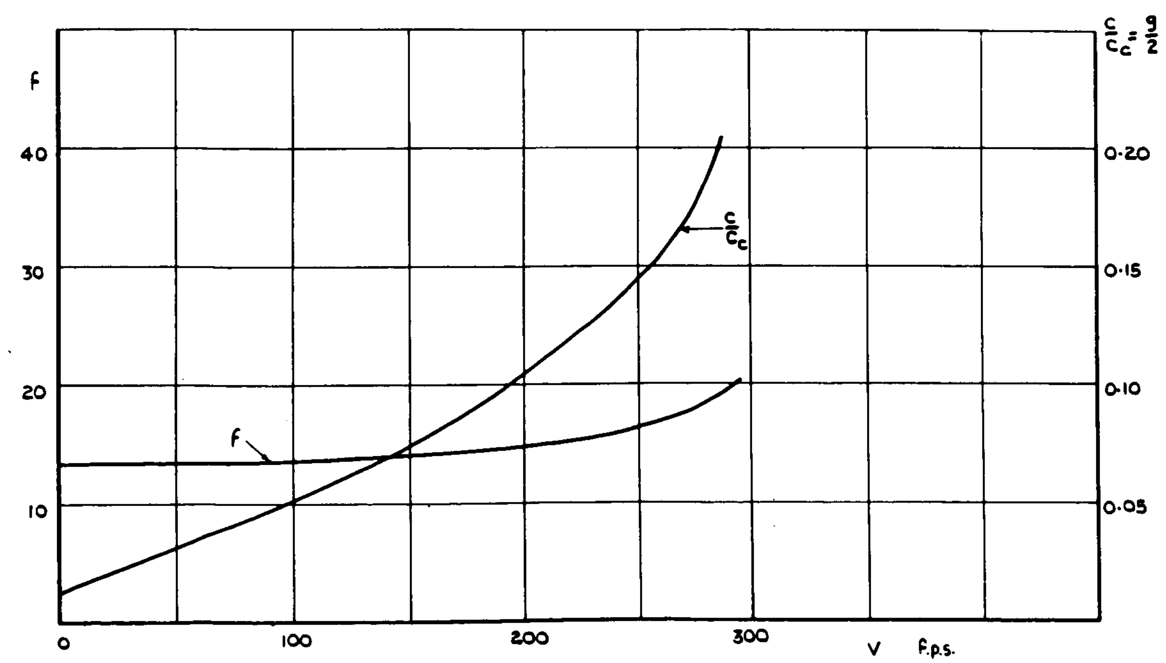

Figure 12. Tailplane Fundamental Symmetric Bending Resonant Frequencies and Damping Against Airspeed

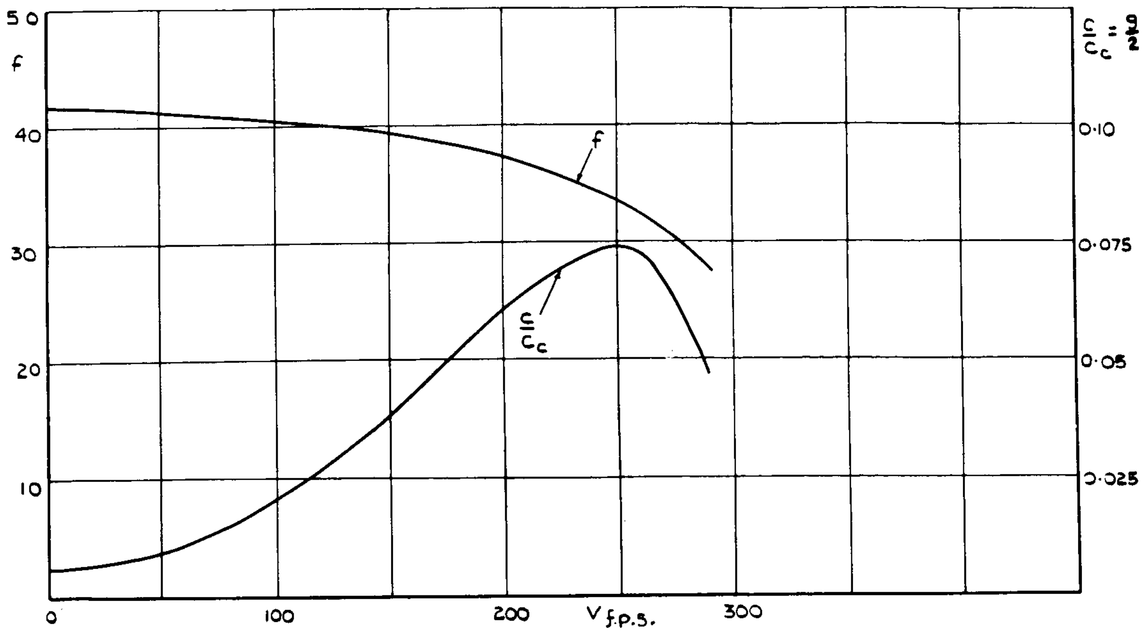

Figure 13. Tailplane Fundamental Symmetric Torsion Resonant Frequencies and Damping Against Airspeed

ACKNOWLEDGEMENT

The author wishes to express his thanks to Bristol Aircraft Limited for making available the results of their wind-tunnel tests, and to Miss E. V. Hartley for carrying out the binary calculations.

LIST OF SYMBOLS

a is an inertia coefficient

d is a damping coefficient

e is an elastic coefficient

g is the phase angle of the restoring force (a damping coefficient)

q is a generalized co-ordinate

F is a generalized exciting force

ω_0 is the natural frequency of one degree of freedom

ω is the exciting frequency

$$\tilde{\omega}^2 = \frac{\omega^2}{\omega_0^2}$$

V_c is the flutter speed

V is the forward speed

$$v = \frac{V}{V_c}$$

List of Symbols (cont)

ν is a frequency parameter $\frac{\omega c}{V_c}$

c is the wing chord

s is the wing span

ρ is the air density

E_{11} is the spring restraint against vertical translation

$$y_0 = \frac{E_{11}}{\rho V_c^2 s c^2}$$

z is vertical displacement

α is the angle of pitch

REFERENCE

Ref. No.	Author	Title, etc.
1	Kennedy, C.C. Pancu, C.D.P.	Use of vectors in vibration measurement and analysis. Journal of the Aeronautical Sciences. Vol. 14, No. 11. November, 1947.